

ADA 041909

C
B.S.



COMPUTER SCIENCE
TECHNICAL REPORT SERIES



DDC
APPROVED
JUL 22 1977
RESOLVED
C

UNIVERSITY OF MARYLAND
COLLEGE PARK, MARYLAND

20742

AD No. _____
DDC FILE COPY

Approved for public release;
Distribution Unlimited

DISTRIBUTION STATEMENT A
Approved for public release;
Distribution Unlimited

14 TR-504
DAAG53-76C-0138

11 February 1977

6 A METHOD OF ADAPTIVE
SMOOTHING AND EDGE ENHANCEMENT.

10 Durga P. Panda
Computer Science Center
University of Maryland
College Park, MD 20742

12 46p.

D D C
RECEIVED
JUL 22 1977
C

9 Technical rept.

ABSTRACT

A local operator, "SWAC", is introduced which identifies image neighborhoods that are noisy and do not contain any boundary. An adaptive smoothing function, guided by the response of SWAC, successfully smooths noisy regions in images without degrading edges. The response of SWAC is also successfully used as a weighting function to suppress spurious responses of an edge detector operating in a noisy environment.

- 1 -

15 The support of the U. S. Army Night Vision Laboratory under ~~DAAG53-76C-0138~~ (ARPA Order-3206) is gratefully acknowledged, as is the help of Mrs. Shelly Rowe. The critical comments of Azriel Rosenfeld, Larry Davis, and David Milgram are deeply appreciated.

DISTRIBUTION STATEMENT A
Approved for public release;
Distribution Unlimited

1472
403018

13

1. Introduction

The presence of random noise in images has two main undesired effects on further utilization of the images. Firstly, the noise makes the image extremely unpleasant to the human visual system (HVS). Secondly, it affects the performance of an automatic image analysis system by giving spurious edge responses at points that really contained no substantial edges in the original (noise-free) image. There are several heuristic as well as mathematically optimal, linear as well as non-linear noise smoothing methods many of which are surveyed in two recent books on picture processing [1 , 2]. Most of the linear methods have space-invariant smoothing point spread functions (PSF) and as a result there is always a trade-off between the degree of smoothing of noise and the degree of blurring of genuine object boundaries. Unless one is willing to post-process the smoothed picture to enhance it and sharpen the edges [3] it may be necessary to use an edge preserving space-variant smoothing method.

One of the pioneering concepts in space-variant smoothing was due to Graham [4]. His method essentially involved smoothing a pixel over a neighborhood that belongs to the same object (or background) region as the pixel itself. This requires determining the object boundaries with reasonable accuracy. Similar methods utilizing various types of edge detector such as the gradient, the Laplacian and the like are conceivable. Examples of recent work of this kind are decision-directed noise smoothing

by Nahi and Habibi [5] and iterative enhancement of noisy images by Lev et al. [6]. Another concept in edge preserving smoothing is the median filter [7]. We investigate here the feasibility of a different approach to adaptive smoothing. The investigation is carried out treating images in only one spatial direction but the extension of the method to two dimensions need not restrict its feasibility. The proposed smoothing method uses a parametric smoothing function, to be described in detail in Section 4, the parameter being constantly updated by computing a certain local measure on the image. The definition of the local measure is based on certain stochastic properties of the random noise.

The second effect of random noise in images can now be reduced in an obvious way, i.e., by detecting edges in the adaptively smoothed image rather than in the noisy image. But, as it turns out, the local measure mentioned above gives us another way of obtaining enhanced edges. If regions that have no edge in the original image, but that contain random noise of magnitude great enough to give false edge response, can be identified, then conceivably the edge response can be modified in such regions to yield a more desirable edge picture.

Let us assume that, in the simplest case, the original image consists of regions of constant gray level, with boundaries between pairs of regions being characterized by abrupt changes in the gray levels ("step edges"). An edge operator such as the maximum absolute difference of

2. A Simple Model

Let us consider a scene of the type described in the previous section in which there are only two regions, each of constant gray level, one region being embedded in or surrounded by the other. The gray level transition from s_0 in the surrounding region, called "background", to s_1 in the embedded region, called "object", is assumed to be abrupt, as described in the earlier section. Let us consider a single row of this scene passing through the object. The gray level $g(i)$ as a function of distance i may appear as shown in Figure 1. In the presence of zero-mean orthogonal noise $n(i)$ the noisy gray levels $x(i)$ in the same row may be as shown in Figure 2.

Figures 3a-c are gray level profiles as viewed through windows of size k points (k assumed odd), centered so that the window is completely in the background region, completely in the object region, and partially in the background and partially in the object region*, respectively. These gray levels, $x'(i)$, are given by

$$x'(i) = x(i+l) \quad (1a)$$

$$x(i) = g(i) + n(i) \quad (1b)$$

where l is the location of the center point of the window.

Now suppose we compute, for each of the three cases

*While Fig. 3c and the corresponding figures in the subsequent analysis show background to object transitions, the existence of similar object to background transitions is understood and implicitly assumed in the analysis.

neighbors, the Roberts cross operator, or the gradient [8 , 2] will yield nonzero response only at the region boundaries. However, the introduction of additive zero-mean orthogonal noise to the noise-free image will yield non-zero responses almost everywhere.

Now suppose that we have a local operator which can discriminate in the noisy picture between neighborhoods that have no gray level transition (no "activity") in the original image and neighborhoods that do have some gray level transition (some "activity") in the original image. This "activity detector" will enable us to suppress the edge response in the neighborhoods of no activity while retaining or enhancing the edge response in the active neighborhoods. A local image operator is presented here that may be used as such an activity detector.

ADDITIONAL INFO

NTIS White Section

DTC Buff Section

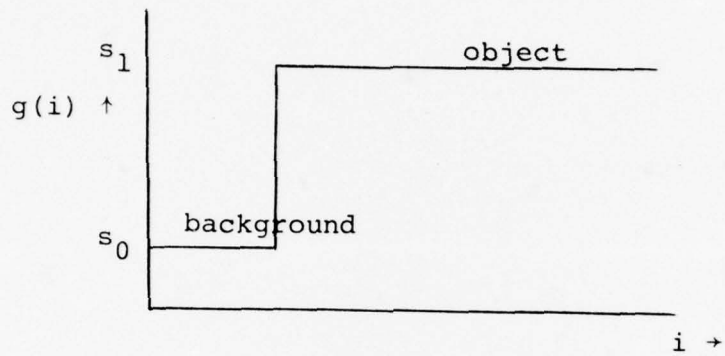
UNANNOUNCED

JUSTIFICATION *See form*

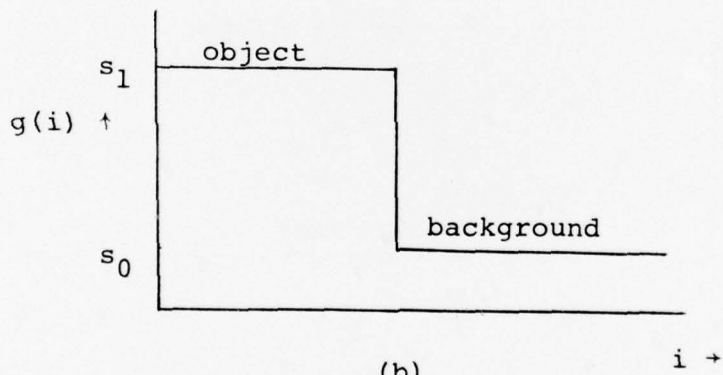
BY *50 file*

DISTRIBUTION/AVAILABILITY CODES

Dist.	AVAIL.	and/or SPECIAL
A		



(a)



(b)

Figure 1

Object and background gray level transition in a noise-free scene.

- a) Background to object transition.
- b) Object to background transition.

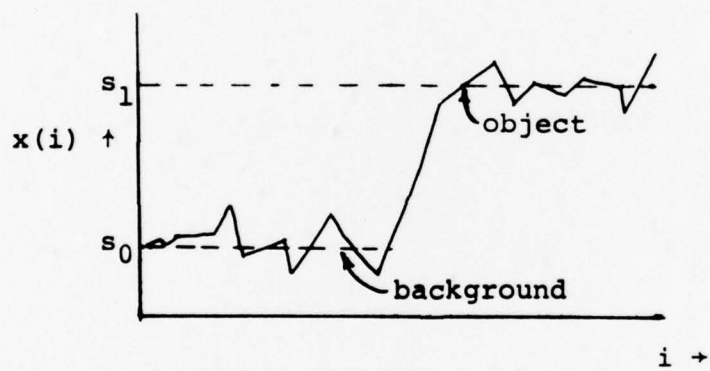


Figure 2

Object and background gray levels in a noisy scene.

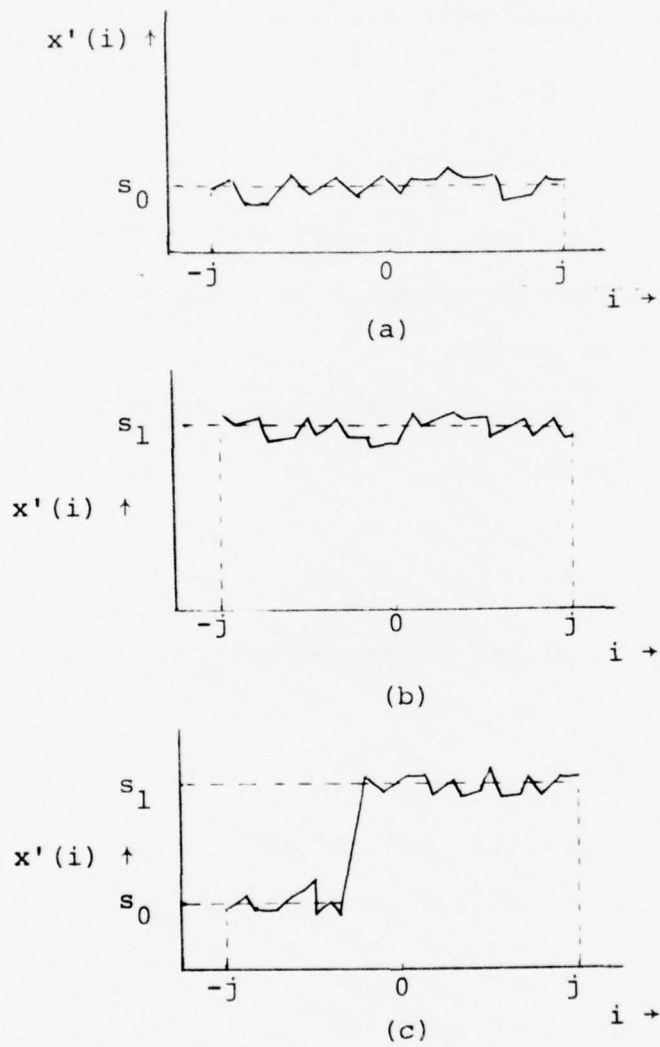


Figure 3

Gray level profiles in windows of size k
 $(j = (k-1)/2)$.

- a. Window located completely in the background.
- b. Window located completely in the object.
- c. Window located partially in the background and partially in the object.

above, the expected gray level of the window and subtract it from the gray level of each point in the window. The transformed gray levels $y(i)$ are given by

$$\begin{aligned} y(i) &= x'(i) - E[x'(i)] \\ &= x(i+l) - E[x(i+l)] \end{aligned} \quad (2)$$

The transformed gray level profiles $y(i)$ in the windows corresponding to those in Figures 3a-c are shown in Figures 4a-c, respectively.

In Figure 4a the window is completely located in the background, therefore

$$x(i+l) = s_0 + n(i+l) \quad (3a)$$

Hence,

$$\begin{aligned} y(i) &= s_0 + n(i+l) - E[s_0 + n(i+l)] \\ &= s_0 + n(i+l) - s_0 \\ &= n(i+l) \end{aligned} \quad (3b)$$

Therefore, the correlation coefficient ρ between two neighboring points in this data sequence $y(i)$ is given by

$$\begin{aligned} \rho &= E[y(i)y(i+1)]/E[y^2(i)] \\ &= E[n(i+l)n(i+l+1)]/E[n^2(i+l)] \\ &= 0/\sigma_n^2 \\ &= 0 \end{aligned} \quad (3c)$$

where σ_n^2 is the variance of the random noise.

Similarly, in Figure 4b the window is completely located in the object region, therefore

$$x(i+l) = s_1 + n(i+l) \quad (4a)$$

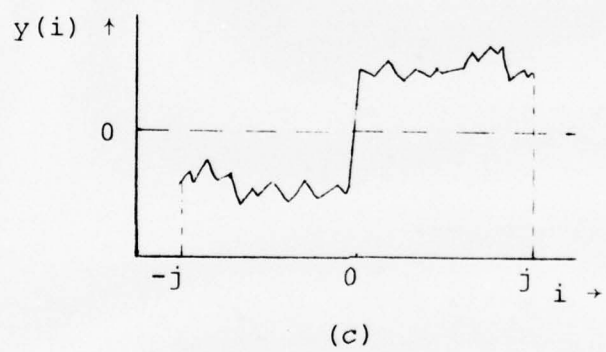
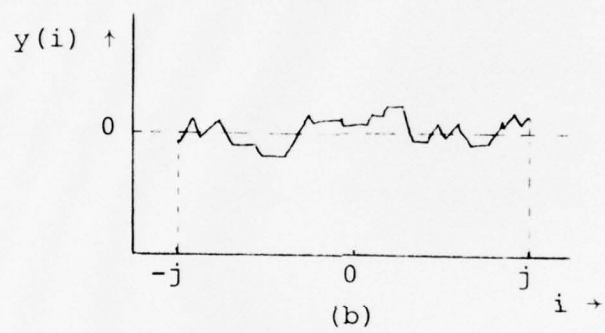
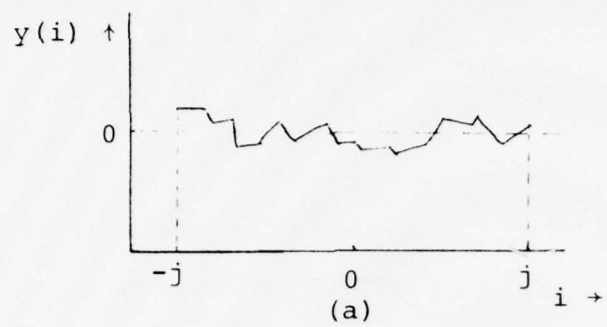


Figure 4

The transformed gray level profiles in the windows of Figures 3a, b, and c.

and

$$\begin{aligned} y(i) &= s_1 + n(i+l) - E[s_1 + n(i+l)] \\ &= n(i+l) \end{aligned} \quad (4b)$$

which again yields

$$\rho = 0 \quad (4c)$$

In Figure 4c, where the window is partially in the background and partially in the object region,

$$x(i+l) = s(i+l) + n(i+l) \quad (5a)$$

$$s(i+l) = s_0 + (s_1 - s_0) \cdot U(\ell') \quad (5b)$$

where $U(\cdot)$ is the unit step function and ℓ' is a random point (assumed uniformly distributed) such that

$$\ell - j \leq \ell' \leq \ell + j. \quad (6)$$

Let the expected value of $s(i+l)$ be μ . Then

$$\begin{aligned} y(i) &= x(i+l) - E[x(i+l)] \\ &= s(i+l) + n(i+l) - E[s(i+l) + n(i+l)] \\ &= s(i+l) - \mu + n(i+l) \\ &= s'(i+l) + n(i+l) \end{aligned} \quad (7)$$

where $s'(i)$ is as shown in Figure 5.

Assuming that $n(i+l)$ is uncorrelated with $s'(i+l)$, the correlation coefficient in the window of Figure 4c is

$$\begin{aligned} &= E[\{s'(i+l) + n(i+l)\}\{s'(i+l+1) + n(i+l+1)\}] / E[\{s'(i+l) + n(i+l)\}^2] \\ &= E[s'(i+l)s'(i+l+1)] / [\sigma_n^2 + E[s'^2(i+l)]] \end{aligned} \quad (8a)$$

It can be shown that for uniformly distributed ℓ' the numerator in eqn. (8a) is always positive and hence

$$\rho > 0. \quad (8b)$$

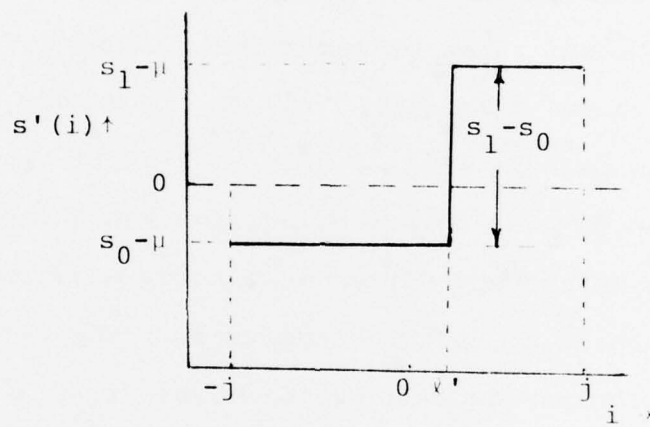


Figure 5

The random sequence $s'(i)$
of eqn. (7).

For uniform ℓ' and large k

$$\Pr\{s(i+\ell) = s(i+\ell+1)\} \gg \Pr\{s(i+\ell) \neq s(i+\ell+1)\} \quad (8c)$$

and hence

$$E[s'(i+\ell) s'(i+\ell+1)] \approx E[s'^2(i+\ell)]. \quad (8d)$$

When the noise is insignificant (small variance) the above ρ is approximately unity. As the noise variance increases the value of ρ goes down, approaching zero for very large noise variance. Hence it is conceivable that the correlation coefficient of sequences of windowed gray levels (with the mean gray level of the window subtracted from the points) will be able to discriminate between neighborhoods near object boundaries and neighborhoods away from object boundaries in a noisy environment. If a window contains an object boundary then the correlation coefficient of the window will be positive. Thus all windows centered within $\pm j$ points of an actual object boundary will be expected to have high correlation coefficients. This implies that a region marked by a high correlation coefficient is k points wide, even though the actual boundary is a step boundary and hence is only one point wide. Hence if we desire to keep the neighborhoods marked by high correlation coefficients restricted to only a few points around the actual object boundary, the window size k must be reduced accordingly.

3. Sample Covariance and Complex Scenes

3.1 A measure of "mean crossing"

In practice the correlation coefficient ρ has to be estimated from the data sequence in the window. A simple estimator of ρ is obtained via the sample window autocorrelation (SWAC) by

$$\hat{\rho} = \left[\frac{1}{k-1} \sum_{i=-j}^{j-1} y(i)y(i+1) \right] / \left[\frac{1}{k} \sum_{i=-j}^j y^2(i) \right]. \quad (9)$$

This estimate, assuming ergodicity, approaches the actual value of ρ if k is large [9].

For $y(i)$ in a neighborhood away from the boundary, as in Figure 4a and b, $y(i)$ may cross zero several times due to the presence of noise. This implies that often $y(i)$ and $y(i+1)$ will have opposite signs, i.e., $y(i)$ is negative and $y(i+1)$ is positive, or vice versa. Thus, while the denominator is always positive, the numerator in eqn. (9) will contain some negative terms and some positive terms. For large k the positive terms may nearly cancel the negative terms to give

$$\hat{\rho} \approx \rho = 0. \quad (10)$$

But if k is small then $\hat{\rho}$ may sometimes have value less than zero, whereas we know that the actual correlation coefficient is zero.

On the other hand, in a neighborhood of the object boundary there may be fewer, most likely only one, zero crossings and hence the value of $\hat{\rho}$ here will be greater than zero. Hence, without loss of any desired information,

the value of $\hat{\rho}$ may be truncated at zero to make the estimate much closer to the actual ρ when k is small. In such a case $\hat{\rho}$ will always yield a value between 0 and 1.

Thus in general if the sequence of gray levels $x'(i)$ in a window (see Figure 3) crosses the mean gray level of the window ("mean-crossing") only a few times relative to k , the value of $\hat{\rho}$ will be high; but if the number of mean-crossings is higher, the value of $\hat{\rho}$ will be closer to zero. We shall denote this truncated local operator $\hat{\rho}$ by SWAC.

3.2 Response of SWAC to a linear boundary

A linear object boundary such as that shown in Figure 6, where the transition between the object gray level and the background level is linear with distance, is a closer approximation to real-life object boundaries than a step edge. In the absence of noise the response of the sample auto-covariance operator to a linear boundary can be analyzed as follows. Let the slope (gray level change per unit distance) of the boundary be $2h$ and let the window of size k be centered at the center of the boundary. After subtracting the window mean the sequence of gray levels $g(i)$ will have values as shown in Figure 7.

Let the width of the boundary be defined as

$$\begin{aligned} w &= (2d+1) + 1 \\ &= 2(d+1) \end{aligned} \quad (11)$$

where d is as shown in Figure 7. Equation (11) implies that the boundary width is an even number of points in the case being considered. We assume that $w < k$. The summation in the denominator in eqn. (9) is

$$\begin{aligned} \sum_{i=-j}^j y^2(i) &= 2n(2(d+1)h)^2 + 2 \sum_{i=1}^d (2hi)^2 \\ &= 8nh^2(d+1)^2 + 8h^2 \sum_{i=1}^d i^2 \end{aligned} \quad (12a)$$

$$\begin{aligned} &= k4h^2(d+1)^2 - (2d+1)4h^2(d+1)^2 + 8h^2 \frac{d(d+1)(2d+1)}{6} \\ &= kh^2w^2 - h^2w^2(w-1) + \frac{h^2}{3}(w-2)(w-1)w \\ &= kh^2w^2 - \frac{2}{3}h^2(w-1)(w+1)w \end{aligned} \quad (12b)$$

where n is as shown in Figure 7. The summation in the

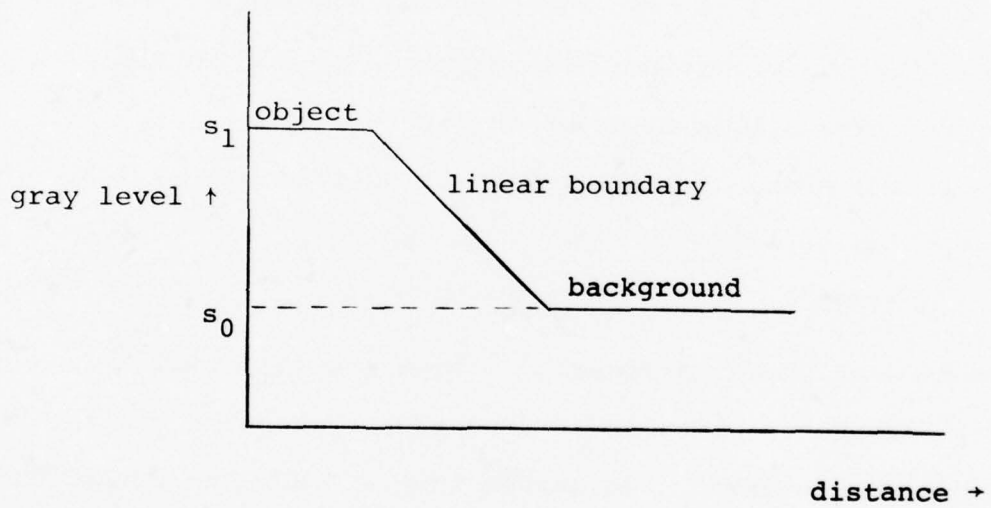


Figure 6

Linear gray level transition at the object boundary.

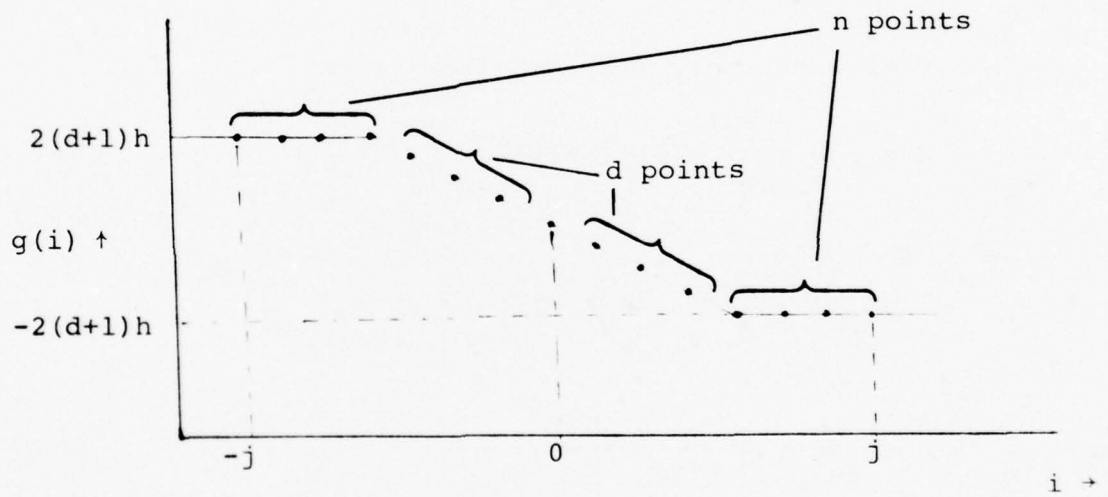


Figure 7

Gray levels at k points symmetrically around the center of a boundary, $k = 2n+2d+1$.

numerator in eqn. (9) is

$$\begin{aligned} \sum_{i=-j}^{j-1} y(i)y(i+1) &= 2(n-1)(2(d+1)h)^2 + 2 \sum_{i=1}^d 4h^2 i(i+1) \\ &= 8nh^2(d+1)^2 - 8h^2(d+1)^2 + 8h^2 \sum_{i=1}^d i^2 + 8h^2 \sum_{i=1}^d i. \end{aligned} \quad (13a)$$

Using eqn. (12a) the above reduces to

$$\begin{aligned} \sum(\cdot) &= \sum_{i=-j}^j y^2(i) - 4h^2(d+1)(d+2) \\ &= \sum_{i=-j}^j y^2(i) - h^2 w(w+2) \end{aligned} \quad (13b)$$

Combining eqns. (12) and (13) we get

$$\begin{aligned} \hat{\rho} &= \frac{k}{k-1} \left[\frac{\sum_{i=-j}^{j-1} y(i)y(i+1)}{\sum_{i=-j}^j y^2(i)} \right] \\ &= \frac{k}{k-1} \left[1 - \frac{3h^2 w(w+2)}{3kh^2 w^2 - 2h^2 w(w-1)(w+1)} \right] \\ &= \frac{k}{k-1} \left[1 - \frac{3(w+2)}{3kw - 2(w^2-1)} \right] \end{aligned} \quad (14)$$

It turns out that we get the same expression for $\hat{\rho}$ when w has an odd number of points. It is obvious from eqn. (14) that the response $\hat{\rho}$ to a linear object boundary is not a function of the slope of the boundary. For this reason $\hat{\rho}$ will perform poorly as an edge detector per se. Also, if the background (or object) region in the original image contains slowly but linearly varying gray level instead of constant gray level then the response of $\hat{\rho}$ in the back-

ground (or object) region will be as high as at the linear object boundary. In the presence of noise, however, if the change in background (or object) region gray level is small enough compared to the amplitude of the noise oscillations, then there will be enough mean-crossing to lower the response $\hat{\rho}$. It is assumed that the slope of the object boundary is high enough so that the amplitude of noise oscillation does not introduce too many additional mean-crossings to lower the response there. Thus, it is expected that even when the object boundary is a ramp, and the background and the object regions are slowly varying rather than constant, the sample auto-covariance operator will be able to discriminate noisy oscillations in regions away from the object boundary.

Table 1 shows the variation of $\hat{\rho}$ with w for various values of k . As it appears from the table for a fixed k the value of $\hat{\rho}$ does not change appreciably for different boundary widths. It is also evident from the table that for a given boundary width, $\hat{\rho}$ increases with k . Hence, to obtain a high response at a boundary, a large k should be chosen. On the other hand, to keep the effect of a boundary on the SWAC response restricted to a small neighborhood around the boundary k should be kept small. It turns out that $k=3$ always results in $\hat{\rho} = 0$ except when the three points in the window have the same gray level. This degenerate case will be avoided in experimentation.

Table 1

w	$\hat{\rho}$				
	k=3	k=5	k=7	k=9	k=11
1	0	.5	.66	.75	.8
2	0	.625	.78	.87	.88
3		.603	.73	.86	.9
4		.5	.78	.86	.9
5			.73	.85	.9
6			.71	.83	.89
7				.79	.88
8				.75	.86
9					.83
10					.8

4. Adaptive Noise Smoothing

This section describes the proposed smoothing method.

The smoothed image $\hat{s}(i)$ is given by

$$\hat{s}(i) = \sum_{\ell=-j}^{j-1} x(i-\ell)h_i(\ell) \quad (15)$$

where $x(\cdot)$ is the gray level of the noisy image and $h_i(\ell)$ is a weighting function that depends on (i) . For a given point (i) we assume that the weighting function is

$$h(\ell) = A e^{-b|\ell|} \quad (16)$$

where A is a normalizing constant that assures that the function $h(\cdot)$ is unimodular, and b is an as yet undetermined parameter whose value depends on (i) . For a given b the smoothing function is purposely designed to resemble the impulse response $h(t)$ of a low pass R-C filter given by

$$h(t) = be^{-bt}U(t) \quad (17)$$

where b is the reciprocal of the R-C circuit time constant and $U(\cdot)$ is the unit step function, required because of the causality restriction. Since image processing does not have any causality restriction, $h(\ell)$ in eqn. (16) has been made a doubly exponential function (for symmetry) while $h(t)$ in eqn. (17) is one-sided exponential.

The parameter b in eqn. (16) is given by

$$b = -\ln(1-\hat{\rho}) \quad (18)$$

where $\hat{\rho}$ is the response of the SWAC operator at the point (i) . In using the definitions of eqn. (16) and (18) it is

assumed that, when $\hat{\rho}=1$ and $\ell=0$

$$(1-\hat{\rho})^{|\ell|} = \lim_{\hat{\rho} \rightarrow 1} (1-\hat{\rho})^0 \quad (19)$$

$$= 1$$

even though 0^0 is actually indeterminate. Thus, if we denote by $\hat{\rho}(i)$ the response of the SWAC operator at the point (i) , then

$$h_i(\ell) = A\{1-\hat{\rho}(i)\}^{|\ell|} \quad (20a)$$

and

$$A = 1 / \sum_{\ell=-j}^j \{1-\hat{\rho}(i)\}^{|\ell|} \quad (20b)$$

Figure 8 shows the function $h_i(\ell)$ without the normalizing constant for various values of $\hat{\rho}$. As can be seen from the figure, when $\hat{\rho}(i)$ is small, implying a noisy background (or object) point, the function is relatively flat. In the limiting case when $\hat{\rho}$ is zero $h_i(\ell)$ is constant at all points, indicating that the smoothed gray level is the local unweighted average of all the k points in the window ("hard smoothing"). On the other hand, when $\hat{\rho}(i)$ is high, implying that the point (i) is in a relatively clean region or in a region with few mean-crossings, the function $h_i(\ell)$ is relatively narrow. In the limiting case when $\hat{\rho}(i)$ is unity, $h_i(\ell)$ is unity at the origin and zero elsewhere, indicating that the smoothed gray level is the same as the original gray level. It may be noted here that $\hat{\rho}(i)$ is unity only when all the points in the window have the same gray level and not when the window is on some object boundary.

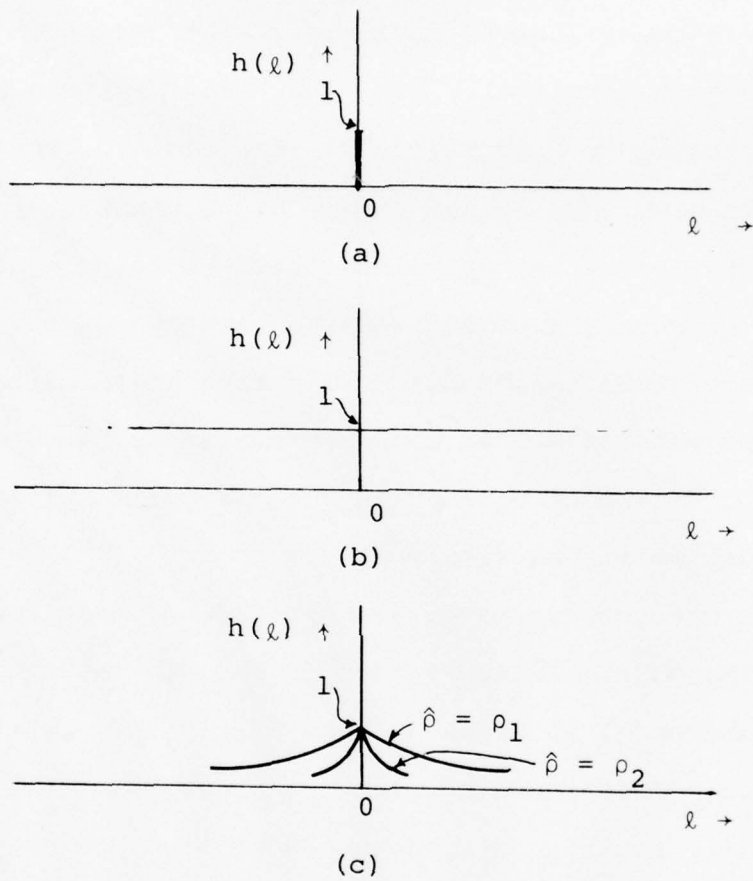


Figure 8

The unnormalized weighting function for various values of $\hat{\rho}(i)$.

- a. $\hat{\rho}=1$
- b. $\hat{\rho}=0$
- c. $0 < \hat{\rho} < 1, \rho_1 < \rho_2$

5. Experimental Results

Four pictures having grayscale 0 to 63 and size 64x64 were selected as test images. The first two pictures show a square object and some chromosomes. The last two pictures are forward looking infrared (FLIR) images of a tank and a truck, respectively. The four test pictures are shown in the top row of Figure 9. The picture "square" is a computer simulated square object of constant gray level embedded in a constant gray level background, with a linear boundary between the object and the background, and zero-mean pseudorandom noise added. The four pictures have various degrees of noise, boundary sharpness, and boundary separation (distance between the center points of two nearest boundaries in the same row).

Next, an edge operator was applied to these four pictures. The edge operator chosen is the DIFF operator, with 2x2 neighborhood, of Hayes and Rosenfeld [10]. It takes the absolute difference between the averages of two horizontally touching neighborhoods of size 2x2 as the edge value $e(i,j)$. Note that the DIFF operator, unlike the SWAC operator, assumes the image to be two-dimensional. There are many edge operators that smooth out the input picture before computing edge values in order to reduce the effect of noise in the edge picture. Such an operator was purposely not chosen here since it was desired to investigate the performance of the SWAC operator in an environment in which the edge response is noisy.

The edge responses for the four test pictures are

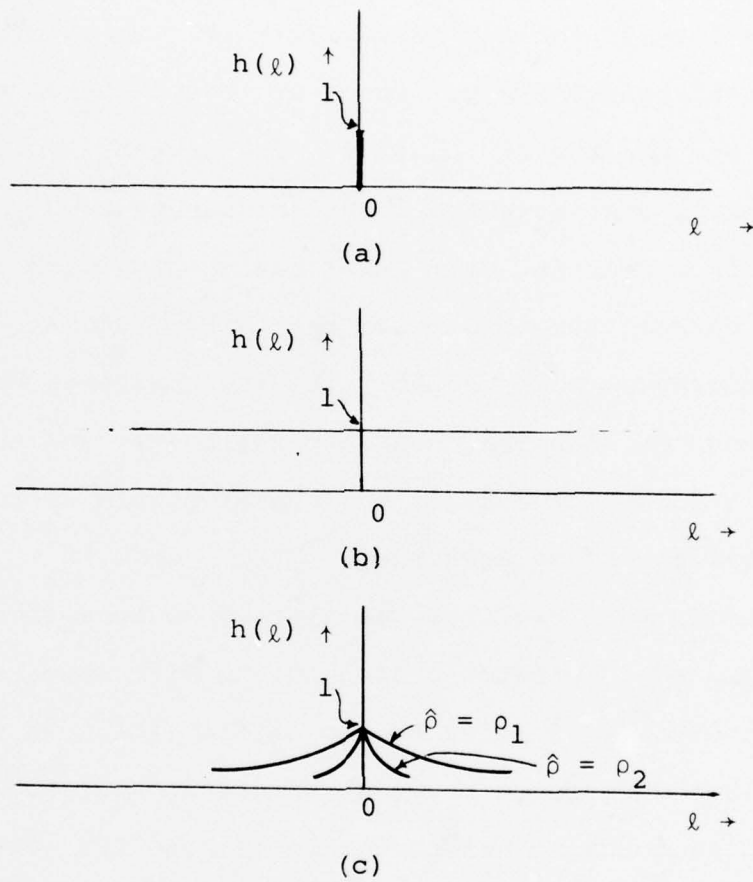


Figure 8

The unnormalized weighting function for various values of $\hat{\rho}(i)$.

- a. $\hat{\rho}=1$
- b. $\hat{\rho}=0$
- c. $0 < \hat{\rho} < 1, \rho_1 < \rho_2$

shown in the second row of Figure 9. As is obvious from Figure 9, the edge operator is certainly one that is sensitive to noise in the input image. The bottom row of Figure 9 shows the same four edge outputs after suppressing the nonmaxima over a four-point horizontal neighborhood. The nonmaximum suppression is done to thin the edges. All the edge pictures in Figure 9 and subsequent figures are stretched to the full grayscale range of 0-63. In Figure 9 as well as in subsequent figures the horizontal sizes of the various pictures seem to be smaller than 64 and to vary from picture to picture. The reason for this is that the response of a local neighborhood operator is not well defined near the border of a picture where the neighborhood falls partially outside the picture. In the case of some operators (e.g., SWAC), the responses at these border points are assumed to have the default value (=0); in the case of other operators (e.g., DIFF), these border points are discarded and the picture size is reduced. Thus in the second and third rows of Figure 9 only 60 columns are displayed; the four border columns have ill-defined responses. For the sake of convenience in display the test pictures in the top row of Figure 9 are also trimmed to 60 columns even though all 64 columns were used in all processing (e.g., DIFF and SWAC).

The SWAC responses for the test pictures were then computed using various window sizes k . The window sizes compared were 5, 7, 9, 11; odd numbers were chosen as window sizes to keep the digital center of the window unique.

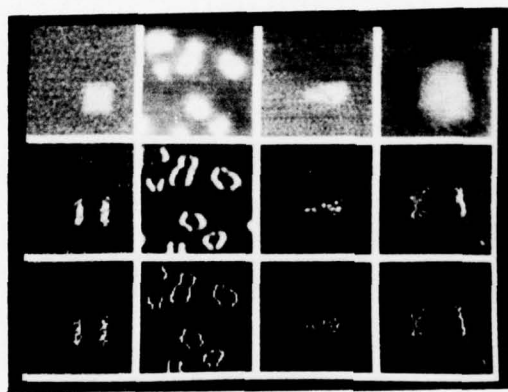


Figure 9

The four test pictures and the edge responses.

row 1: The test pictures.

row 2: The edge (2x2 DIFF) response for the test pictures.

row 3: Local maxima over 4 horizontal neighbors of the DIFF pictures.

column 1: the square

column 2: the chromosomes

column 3: the tank

column 4: the truck

The SWAC image for each of the above four values of k are shown in Figure 10. For $k=11$ the object boundaries are outlined in the SWAC pictures of the square, the chromosomes and the truck by very thick curves (first row of Figure 10). It may be mentioned here that since the SWAC operator is one-dimensional and operates on a row of picture at a time the horizontal components of the boundaries are not outlined in the SWAC images. The reason for getting thick outlines of the boundaries is, as mentioned in Section 2, that the response due to a boundary is expected to spread j points to the left and to the right of the actual boundary. For this reason, in the SWAC responses of the tank where boundary separations are smaller, the responses from various boundaries overlap and hence do not outline the actual object boundaries.

The noise smoothing of the test pictures was done by using the SWAC response, $\hat{\rho}$, displayed in Figure 10 and the smoothing function of eqn. (20). Obviously, for each k , eqn. (20) yields one set of smoothing functions and this yields one set of smoothed images. Figure 11 shows the smoothed test pictures for $k = 5, 7, 9, 11$. It is clear from Figure 11 that, for all the four values of k , the test pictures are adequately smoothed without any visible degradation of the object boundaries. The only visibly unpleasant effects in the smoothed pictures are the occasional horizontal "streaks" which are due to the fact that the smoothing operation is one-dimensional. To highlight the performance of the adaptive smoothing method the adap-

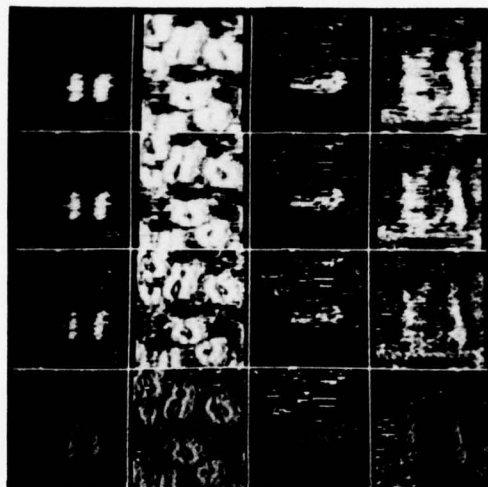


Figure 10

The SWAC responses for various k's and various test pictures.

row 1: k=11
row 2: k=9
row 3: k=7
row 4: k=5

column 1: the square
column 2: the chromosomes
column 3: the tank
column 4: the truck

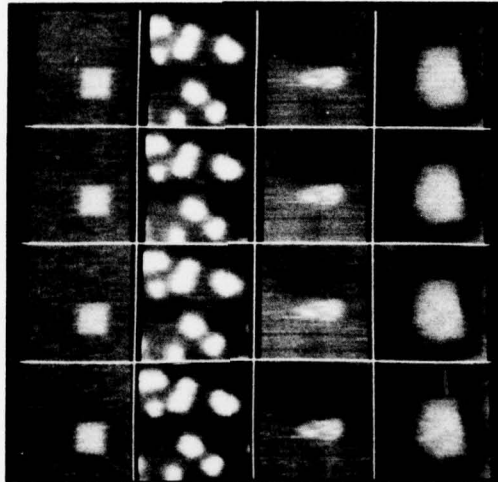


Figure 11

Adaptive smoothing of the test pictures for various k's.

row 1: k=11
row 2: k=9
row 3: k=7
row 4: k=5

column 1: the square
column 2: the chromosomes
column 3: the tank
column 4: the truck

tively smoothed pictures for $k=11$ are compared with the test pictures smoothed by a local unweighted averaging, a common method, over the same neighborhood size. The results for adaptive smoothing and local averaging are shown one above another in the top two rows of Figure 12. The bottom two rows of Figure 12 show the result of edge detection, using the same DIFF operator as in the middle row of Figure 9. The relatively thin and noise-free edges in the third row of Figure 12 are due to adaptive smoothing. The thick edges in the bottom row of the same figure are due to local averaging. Also evident from the bottom two rows of Figure 12 is the fact that the highest edge responses in the averaged pictures are not as strong compared to the false responses in the backgrounds as they are in the case of the adaptive smoothing.

A more detailed comparison of the adaptive smoothing method with local averaging or median filtering is desirable. Where an automatic image analysis system is used it may be of interest to compare the improvement in the performance of the system under the various smoothing techniques. A theoretical analysis of the performance of the adaptive smoothing method would also be desirable. The criterion of performance must take into account error in the edge value as well as the error in the gray level of the output picture.

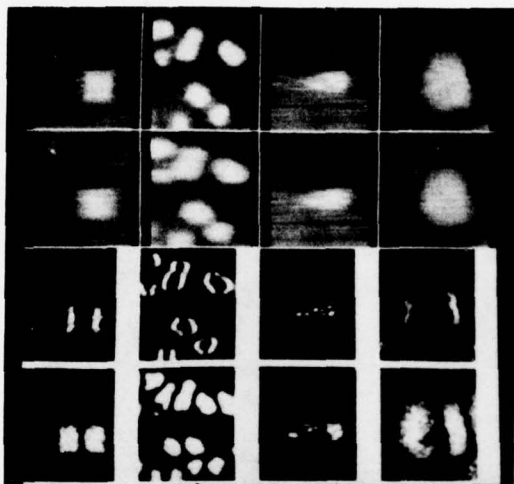


Figure 12

Comparison of the adaptive smoothing and local averaging for $k=11$.

- row 1: The test pictures smoothed adaptively.
- row 2: The test pictures locally averaged.
- row 3: The edge (DIFF) responses for the pictures in row 1.
- row 4: The edge (DIFF) responses for the pictures in row 2.

- column 1: the square
- column 2: the chromosomes
- column 3: the tank
- column 4: the truck

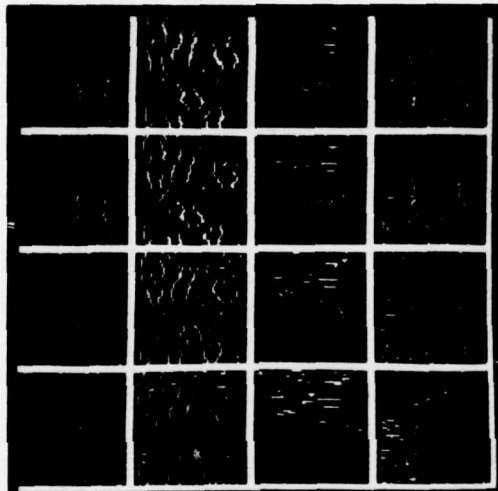


Figure 13

Nonmaxima suppressed SWAC responses for various k's.

row 1: k=11
row 2: k=9
row 3: k=7
row 4: k=5

column 1: the square
column 2: the chromosomes
column 3: the tank
column 4: the truck

To investigate the possibility of SWAC as an edge operator, local nonmaximum suppression was performed on the SWAC images. The result is shown in Figure 13. When an edge thinning operation such as nonmaximum suppression is applied to the SWAC pictures it yields many spurious responses in the background, and in all except the chromosome pictures it produces sets of discontinuous edge points, but no sharp thin outlines at the object boundaries. In the case of the chromosomes, where the boundaries are sharp and the background is noise-free, non-maximum suppression yields thin connected curves outlining the object boundaries. The same phenomenon may also be observed for $k = 5, 7,$ and 9 .

Comparing various rows of Figure 10 it may be observed that while a smaller k gives thinner object boundary outlines, it also gives, as predicted in Section 3.2, weaker responses at the object boundaries (see, for example, the chromosomes picture) and large streaks of spurious high response (the white lines in the Figures) in the backgrounds. The spurious streaks are due to the fact that often there are small sets of neighboring points in the backgrounds that have a constant gray level and hence appear noise-free in a smaller window, but increasing the window size brings in more neighboring points that make the noise evident.

A weighted edge response for each of the test pictures was computed next by using the SWAC response at a point

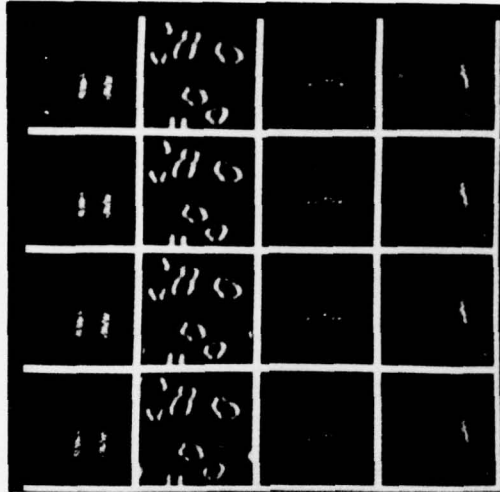


Figure 14

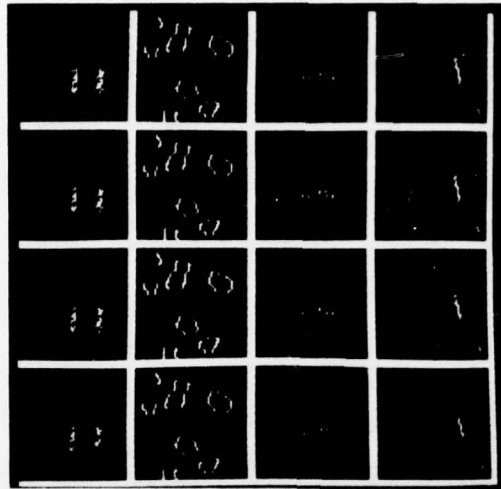
The weighted edge responses for various test pictures
and various k's.

row 1: k=11
row 2: k=9
row 3: k=7
row 4: k=5

column 1: the square
column 2: the chromosomes
column 3: the tank
column 4: the truck

(i,j) as the a posteriori weighting coefficient of the edge response $e(i,j)$ at that point. The effect of this weighting is expected to be, as mentioned earlier, to attenuate the noisy responses in the noisy background regions and to relatively enhance the edge responses in the neighborhoods of the object boundaries. The results of this weighting for various values of k are shown in Figure 14. The weighted edge gives fairly high responses at the object boundaries and relatively insignificant false responses in the background. In the chromosomes picture, where the unweighted edge picture is practically noise-free, the weighted edge pictures also have sharp noise-free edges at the boundaries. Thus, while the SWAC operation discriminates against noise, it has no adverse effect on noise-free images. There is no trade-off in SWAC performance as in, for example, edge detection by the absolute difference of window means, where the effect of background noise is reduced at the cost of thickening the edge responses at the object boundaries.

The SWAC response may also be used as an a posteriori weighting coefficient of nonmaxima suppressed edge (DIFF) responses. Figure 15a shows the result of doing this for $k = 5, 7, 9,$ and 11 . Even though many of the edges in Figure 15a are thin, and of course noise-free, there seems to be a high risk of losing continuity in the edges. Figures 15b and 15c show the result of using nonmaxima suppressed SWAC responses as the a posteriori weighting coefficients of edge pictures and nonmaxima suppressed edge



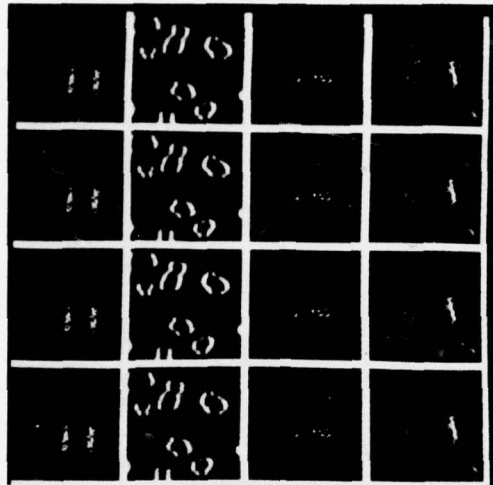
(a)

Figure 15

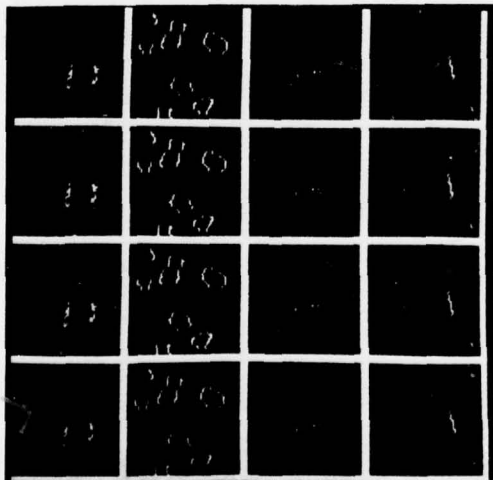
The effects on weighted edge response of nonmaxima suppression at various stages.

- (a) nonmaxima suppression of the unweighted edges
- (b) nonmaxima suppression of the SWAC responses
- (c) nonmaxima suppression of both the unweighted edges and the SWAC

row 1: k=11	column 1: the square
row 2: k=9	column 2: the chromosomes
row 3: k=7	column 3: the tank
row 4: k=5	column 4: the truck



(b)

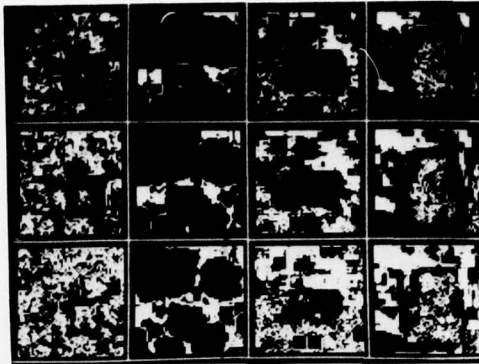


(c)

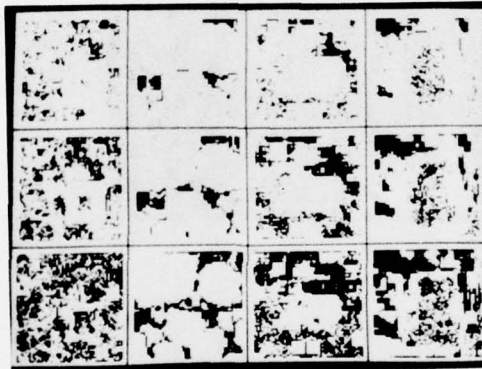
Figure 15 (cont'd)

pictures, respectively. Among Figures 14, 15a, 15b, and 15c, Figure 14 seems to have the most desirable edge pictures.

It is conceivable that the false edge responses in noisy backgrounds (or object interiors) can be suppressed by some method other than a measure of the degree of "noisiness" in a neighborhood. A segmentation procedure based on statistical hypothesis testing [11] was used to determine if a neighborhood of a certain size around each point belongs to a single region, such as background, or to more than one region, as when the point is at or near an object boundary. The four test pictures segmented by the above hypothesis test are shown in Figure 16. In Figure 16a the dark points (gray level zero) are where the null hypothesis, that a neighborhood of size $k \times k$ around the point belongs to a single population, was rejected. The confidence level and the ratio of the number of intervals to the sample standard deviation of the neighborhood were 0.99 and 1.8, respectively (see [11] for the meanings and the importance of these quantities). Figure 16b is the negative of Figure 16a. The top, the middle, and the bottom rows of Figure 16 correspond to neighborhood sizes of 11×11 , 9×9 , and 7×7 , respectively. When the gray levels in Figure 16b are used as the point-wise weighting coefficients to construct weighted edge pictures from DIFF responses (Figure 9, 2nd row) it results in very insignificant, if any, noise suppression and edge enhancement. The resulting weighted edge pictures are shown in Figure 17.



(a)



(b)

Figure 16

Segmentation by the hypothesis test.

(a) dark points are rejected points

(b) the negative of (a)

row 1: neighborhood size 11x11

row 2: neighborhood size 9x9

row 3: neighborhood size 7x7

column 1: the square

column 2: the chromosomes

column 3: the tank

column 4: the truck

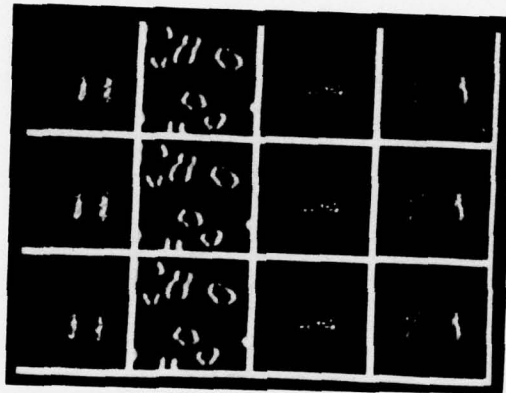


Figure 17

The weighted edge pictures using the hypothesis test with $k \times k$ neighborhoods.

row 1: $k=11$
row 2: $k=9$
row 3: $k=7$

column 1: the square
column 2: the chromosomes
column 3: the tank
column 4: the truck

6. Conclusions

The performance of the adaptive smoothing method on the test pictures is excellent in the sense that the smoothed pictures have noise suppressed extremely well and have no apparent degradation of object boundaries. The thicknesses of the edges detected by the DIFF operator before and after adaptive smoothing are seen to be the same. The smoothing method is based on a very simple concept of measuring the degree of noisiness in a neighborhood. The SWAC noise measure is motivated by the stochastic property of the noise, namely that it is orthogonal. Even though the sample size, k , is too small from the point of view of statistics, the effectiveness of the measure in guiding the adaptive smoothing function is impressive. The degree of smoothing is reduced not only near the object boundaries, as in Graham's method [4], but also in regions that do not contain appreciable noise. Even if a very simple image model is used in the theoretical analysis, the effectiveness of the smoothing method seems to extend to almost any picture. The method does not require any a priori knowledge, such as noise variance, or any knowledge of statistics of edge values in the picture that may be required by an edge-detection oriented smoothing method (e.g., [4]). It appears that variation of k , the operator size, does not make much difference in the smoothed pictures.

The operator SWAC also gives us a systematic way of reducing false response in edge pictures. The response of the SWAC operator, when used as an a posteriori weighting

of an otherwise noisy edge detector, discriminates against background noise in noisy pictures and enhances genuine edge responses at the actual object boundaries without thickening the boundary outlines or having any adverse effect on noise-free images. It appears that there is not much difference in the weighted edge pictures for various window sizes. A smaller window size, while involves less computation, outlines the well-separated object boundaries with relatively thinner lines. It should be borne in mind that the types of scenes considered in the analysis as well as in the experiments do not have any textural detail.

It may be argued that the false response of any edge detector can be reduced by weighting it with the response of another "orthogonal" edge detector. Such a method will solely rely on the fact that the false responses of two different edge operators may (hopefully) not lie at the same points. On the other hand a method based on gray level statistics will require, and be valid over, large neighborhoods. One disadvantage of large neighborhood size is the loss of resolution, such as in the top two rows of Figures 16a and 16b, exemplifying the result of the hypothesis test. This is one disadvantage that the method based on SWAC does not suffer from.

References

1. T. S. Huang (ed.), Picture Processing and Digital Filtering, Springer-Verlag, 1975.
2. A. Rosenfeld and A. C. Kak, Digital Picture Processing, Academic Press, 1976.
3. D. P. Panda and A. C. Kak, Image restoration and enhancement, Tech. Rept. TR-EE 76-17, Purdue University, W. Lafayette, Indiana, June 1976.
4. R. E. Graham, "Snow removal - a noise stripping process for picture signals", IRE Trans. on Inf. Th. pp. 127-144, February 1962.
5. N. E. Nahi and A. Habibi, "Decision-directed recursive image enhancement", IEEE Trans. on Ckt. and Syst. vol. CAS-22, no. 3, pp. 286-293, March 1975.
6. Amos Lev, Steven W. Zucker and Azriel Rosenfeld, "Iterative enhancement of noisy images" to be published in IEEE Trans. on Syst. Man, and Cyber.
7. B. R. Frieden, "A new restoration algorithm for the preferential enhancement of edge gradients", in Image Processing, Proc. SPIE, Pacific Grove, California, pp. 44-48, February 1976.
8. R. O. Duda and P. E. Hart, Pattern Classification and Scene Analysis, Wiley, 1973.
9. A. Papoulis, Probability, Random Variables, and Stochastic Processes, McGraw-Hill, 1965.
10. K. C. Hayes, Jr. and A. Rosenfeld, Efficient edge detectors and applications, Comp. Sc. Center, Univ. of Maryland, College Park, Maryland, Tech. Rep. 207, November 1972.
11. N. Ahuja, L. S. Davis, D. L. Milgram, and A. Rosenfeld, Piecewise approximation of pictures: further experiments, Comp. Sc. Center, Univ. of Maryland, College Park, Maryland, Tech. Rep. 462, July 1976.

UNCLASSIFIED

SECURITY CLASSIFICATION OF THIS PAGE (When Data Entered)

REPORT DOCUMENTATION PAGE		READ INSTRUCTIONS BEFORE COMPLETING FORM
1. REPORT NUMBER	2. GOVT ACCESSION NO.	3. RECIPIENT'S CATALOG NUMBER
4. TITLE (and Subtitle) A METHOD OF ADAPTIVE SMOOTHING AND EDGE ENHANCEMENT		5. TYPE OF REPORT & PERIOD COVERED Technical
7. AUTHOR(s) Durga P. Panda		6. PERFORMING ORG. REPORT NUMBER TR-504
9. PERFORMING ORGANIZATION NAME AND ADDRESS Computer Science Ctr. Univ. of Maryland College Park, MD 20742		8. CONTRACT OR GRANT NUMBER(s) DAAG53-76C-0138
11. CONTROLLING OFFICE NAME AND ADDRESS U.S. Army Night Vision Lab. Ft. Belvoir, VA 22060		10. PROGRAM ELEMENT, PROJECT, TASK AREA & WORK UNIT NUMBERS
14. MONITORING AGENCY NAME & ADDRESS (if different from Controlling Office)		12. REPORT DATE February 1977
		13. NUMBER OF PAGES
		15. SECURITY CLASS. (of this report) Unclassified
		15a. DECLASSIFICATION/DOWNGRADING SCHEDULE
16. DISTRIBUTION STATEMENT (of this Report) Approved for public release; distribution unlimited.		
17. DISTRIBUTION STATEMENT (of the abstract entered in Block 20, if different from Report)		
18. SUPPLEMENTARY NOTES		
19. KEY WORDS (Continue on reverse side if necessary and identify by block number) Image enhancement Smoothing Edge detection		
20. ABSTRACT (Continue on reverse side if necessary and identify by block number) A local operator, "SWAC", is introduced which identifies image neighborhoods that are noisy and do not contain any boundary. An adaptive smoothing function, guided by the response of SWAC, successfully smooths noisy regions in images without degrading edges. The response of SWAC is also successfully used as a weighting function to suppress spurious responses of an edge detector operating in a noisy environment.		

DD FORM 1473 1 JAN 73 EDITION OF 1 NOV 65 IS OBSOLETE

UNCLASSIFIED

SECURITY CLASSIFICATION OF THIS PAGE (When Data Entered)